2018

Carbon fluxes and interannual drivers in a temperate forest ecosystem assessed through comparison of top-down and bottom-up approaches

Andrew P. Ouimette
University of New Hampshire

Scott V. Ollinger
University of New Hampshire

Andrew D. Richardson
Harvard University

David Y. Hollinger
USDA Forest Service Northern Research Station

Trevor F. Keenan
Lawrence Berkeley National Lab

Recommended Citation
Ouimette, AP, Ollinger SV, Richardson AD, Hollinger DY, Keenan TF, Lepine LC, and Vadeboncoeur MA. 2018. Carbon fluxes and interannual drivers in a temperate forest ecosystem assessed through comparison of top-down and bottom-up approaches. Agricultural and Forest Meteorology 256–257: 420–430.

Carbon fluxes and interannual drivers in a temperate forest ecosystem assessed through comparison of top-down and bottom-up approaches

Andrew P. Ouimette[a]*, Scott V. Ollinger[a], Andrew D. Richardson[b], David Y. Hollinger[c], Trevor F. Keenan[d], Lucie C. Lepine[a], Matthew A. Vadeboncoeur[a]

[a] University of New Hampshire, Earth Systems Research Center, Durham, NH 03824

[b] Harvard University, Department of Organismic and Evolutionary Biology, Cambridge MA 02138

[c] USDA Forest Service, Northern Research Station, 271 Mast Rd, Durham, NH 03824

[d] Earth Sciences Division, Lawrence Berkeley National Lab, Berkeley, CA 94709, USA

Abstract

Despite decades of research, gaining a comprehensive understanding of carbon (C) cycling in forests remains a considerable challenge. Uncertainties stem from persistent methodological limitations and the difficulty of resolving top-down estimates of ecosystem C exchange with bottom-up measurements of individual pools and fluxes. To address this, we derived estimates and associated uncertainties of ecosystem C fluxes for a 100-125 year old mixed temperate forest stand at the Bartlett Experimental Forest, New Hampshire, USA, using three different approaches: (1) tower-based eddy covariance, (2) a biometric approach involving C flux measurements of individual ecosystem subcomponents, and (3) an inventory approach involving changes in major C stocks over time. Our analysis made use of 13 years of data, collected over the period from 2004 to 2016.

Estimates of mean annual net ecosystem production (NEP) ranged from 120-133 g C m^{-2}, demonstrating strong agreement among methods and suggesting that this aging forest acts as a moderate C sink. The use of multiple approaches to measure C fluxes and their uncertainties helped place constraints on difficult-to-measure processes such as aboveground contributions to ecosystem respiration and belowground allocation to mycorrhizal fungal biomass (which was estimated at 20% of net primary production).

Analysis of interannual variability in C fluxes revealed a decoupling between annual wood growth and either current year or lagged NEP or GPP, suggesting that source limitation (C supply) is likely not controlling rates of wood production, at least on an interannual scale. Results also demonstrated a strong association between the maximum rate of C uptake during the growing season (Amax) and the length of the

vernal window, defined as the period of time between soil thaw and the onset of photosynthesis. This suggests an important, but poorly understood, influence of winter and spring climate on mid-summer canopy physiology. Efforts to resolve the mechanisms responsible should be prioritized in light of ongoing and predicted changes in climate for the northeastern U.S. region, particularly during the winter and winter-spring transition period.

*Corresponding author; Andrew.Ouimette@unh.edu

1. Introduction

Forests represent the dominant land cover type in the northeastern United States (Foster and Aber. 2004) and are widely regarded as carbon sinks given their state of recovery from widespread agriculture in the 19th century (Caspersen et al., 2000; Goodale et al., 2002). However, the ability of these aging secondary forests to continue to act as net carbon sinks as they transition to late-successional stands is unclear. Although a commonly accepted view is that old-growth forests are carbon neutral (Odum, 1969), more recent reviews indicate that late successional forests can often act as net carbon sinks (Luyssaert et al., 2008). Additional data on the net carbon flux of eastern North American forests should improve our understanding of the ability of these forests to continue to act as net carbon sinks.

Approaches to estimating net C exchange in forests include eddy covariance flux towers, biometric estimates of growth and respiration, and changes in important C stocks over time. Each of these has inherent strengths and limitations. Eddy flux towers provide direct measurements of net CO_2 exchange at high temporal resolution, but can suffer from unquantified advective losses (e.g. Aubinet et al., 2012; Novick et al., 2014; van Gorsel et al., 2009; Vickers et al., 2012), data gaps during calm periods, and non-CO_2 C fluxes. Eddy flux measurements also lack information on how C is allocated to various ecosystem components (e.g. foliage, wood, fine roots, mycorrhizal fungi), that possess a range of functions and C residence times and that are required to more fully test ecosystem models.

Biometric approaches that quantify the difference between net primary production (NPP) and heterotrophic respiration (R_h), can provide independent estimates of net

ecosystem C exchange and can shed light on how C is allocated among various pools. However, this requires estimates of difficult-to-measure fluxes (e.g. belowground biomass production), which can introduce substantial uncertainties (Clark et al., 2001)

Estimating net C exchange from changes in major C stocks offer yet another approach, the benefits of which include its straightforward nature and lack of reliance on difficult-to-measure fluxes. However, belowground C pools are large and notoriously variable, making change detection extremely difficult (Vadeboncoeur et al., 2012). And, on its own, this method doesn't offer insight into mechanisms or subcomponent C fluxes. Consistency between top-down and bottom-up C quantification approaches can greatly enhance confidence in estimates of an ecosystem's C balance. Taken together, data from multiple approaches can also provide estimates on a full suite of ecosystem C fluxes to which ecosystem models can be more thoroughly compared.

Here we used multiple methodological approaches to compile a comprehensive carbon budget for an aging (100-125 year old) mixed temperate forest in New England (Bartlett Experimental Forest, NH). This included a comparison of net and gross ecosystem C fluxes using 3 complementary approaches (eddy covariance, biometric estimates of NPP and R_h, and a modified C inventory approach) for 13 years (2004-2016) of data. We included estimates of uncertainty for all three approaches, and highlight how the comparison of several independent methodological approaches provided more confidence in estimates of difficult-to-measure respiratory and belowground fluxes. Finally, drivers of interannual variations of C fluxes were evaluated by comparing net ecosystem production (NEP), gross primary production (GPP), ecosystem respiration (Re), and wood growth to an array of climatic, phenological, and biological variables.

2. Methods

2.1. Site description

Bartlett Experimental Forest (BEF) (44°06'N, 71°3'W) is located within the White Mountain National Forest in north-central New Hampshire, USA (Figure 1). The climate is humid continental with cool summers (mean July temperature, 19°C) and cold winters (mean January temperature, –9°C). Mean annual temperature is 6°C and mean annual precipitation is 1270 mm (for additional site information, see http://www.fs.fed.us/ne/durham/4155/bartlett.htm). The forest within the eddy covariance tower footprint was cutover circa 1900 and some areas were damaged by the 1938 hurricane. In the past decade there has also been small-scale forest management just outside the tower footprint, but mean stand age is roughly 100-125 years. Average canopy height is approximately 20–22 m within the tower footprint and is composed of a diverse assemblage of species including *Acer rubrum* (29%), *Fagus grandifolia* (25%), *Tsuga canadensis* (14%), *Betula alleghaniensis* (9%), *Betula papyrifera* (6%), *Fraxinus americana* (5%), *Acer saccharum* (5%), and *Populus grandidentata* (4%), with minor amounts of other coniferous species. Soils are generally acidic Spodosols and Inceptisols derived from granitic till, and poor in both Ca and P (Vadeboncoeur et al., 2014). Foliar N and ecosystem N cycling rates are both low relative to other mixed hardwood sites in the region (Ollinger et al., 2002).

In 2003, BEF was adopted as a NASA North American Carbon Program (NACP) Tier-2 field research and validation site. During this time a 26.5 m tower was installed in a low-elevation (290 m) mixed hardwood stand for the purpose of making eddy

covariance measurements of the forest–atmosphere exchange of carbon dioxide, water, and sensible heat. Continuous flux and meteorological measurements began in January, 2004 and are ongoing (data are available online from AmeriFlux, http://www.public.ornl.gov/ameriflux/). In 2004, 12 FIA-style plots (Hollinger, 2008) were established across a 1 km by 1 km area centered on the flux tower for the purpose of making complimentary biometric measurements of carbon pools and fluxes. BEF is also a NEON relocatable site (construction began in the summer of 2013) and the new flux tower is located within 100 meters of the existing flux tower.

2.2. Eddy covariance estimates of C flux and uncertainty

The eddy covariance system provides direct measurements of the net ecosystem exchange rate of CO_2 between the forest canopy and the atmosphere (NEE). Eddy covariance estimates of NEE, after accounting for a change in sign, are equivalent to net ecosystem production (NEP_{EC}) assuming that sources and sinks of inorganic C are negligible (Chapin III et al., 2006).

Forest–atmosphere CO_2 flux (NEE) was measured at a height of 25 m with an eddy covariance system consisting of a model SAT-211/3K 3- axis sonic anemometer (Applied Technologies, Longmont, Colo.) and ducted to a model LI-6262 CO_2/H_2O infrared gas analyzer (Li-Cor, Lincoln, Neb.), through 2500 cm of 0.476 cm ID polyethylene tubing at 75 cc s^{-1} with data recorded at 5 Hz and fluxes (covariances) calculated every 30 minutes. In 2014 the LI-6262 was replaced with a model LI-7200 analyzer. Average (30 minute) meteorological variables (e.g. air and soil temperatures, incoming solar radiation, etc.) measured at the tower were recorded concurrently. The instrument configuration, calibration protocol, QA/QC, and data processing procedures

were identical to those used at the Howland AmeriFlux site in central Maine, USA, and have been documented in detail elsewhere (Hollinger et al., 2004). Site visits by the AmeriFlux Tech Team took place in the summers 2006 and 2016, to confirm overall quality of the flux and meteorological measurements.

Half-hourly NEE data were filtered to remove time periods with low atmospheric turbulence where advective losses were likely significant similar to Barr et al. (2013). Following this approach a median ustar threshold of 0.50 ± 0.10 was detected and used across all seasons and years. Gaps in NEE were filled using the (Barr et al., 2004) Fluxnet-Canada method (FCM) with slight modifications, including: mild exclusion of NEE outliers; use of a weighted mean of soil and air temperature as the independent variable for estimating Re; and delineation of nighttime periods from global shortwave radiation of less than 5 W m^2. Random uncertainties in NEE were estimated following (Richardson and Hollinger, 2007). NEE was partitioned into gross primary production (GPP_{EC}) and total ecosystem respiration (Re_{EC}) using the FCM method. Further details of the gap-filling an partitioning methods used are presented in Barr et al. (2013).

2.3. Biometric estimates of carbon fluxes with uncertainty

In addition to eddy covariance, we used measurements of individual ecosystem components to make biometric estimates of gross and net carbon fluxes. For biometric estimates of NEP, (NEP_B), we subtracted heterotrophic respiration (R_h), including respiration from dead woody biomass (R_{DW}), and the heterotrophic portion of soil respiration (R_{SH}), from total net primary production (NPP), including NPP from foliage, aboveground woody tissues, understory production, fine and coarse roots, and mycorrhizae (Table 1). We also calculated biometric estimates of gross primary

146 production (GPP_B) and ecosystem respiration (Re_B). GPP_B was calculated by summing
147 all sources of NPP, with all sources of autotrophic respiration, including autotrophic
148 respiration from foliage, aboveground wood, and the autotrophic portion of soil
149 respiration (Table 1). Biometric estimates of Re_B were calculated by summing all
150 sources of heterotrophic and autotrophic respiration including total soil respiration,
151 respiration from coarse woody debris and standing dead wood, as well as from foliar and
152 woody tissues.

153 **2.3.1. Aboveground production**

154 Beginning in 2004 estimates of aboveground carbon pools and fluxes were made on 12
155 plots within a 1 km by 1 km area centered on the flux tower with a similar layout, but
156 larger size, to that described in Hollinger (2008). Each of the 12 plots contains four 10 m
157 radius subplots for a total of 48 subplots within the 1 km^2 footprint of the flux tower.
158 Each subplot contains 3 soil respiration collars, 2 litterfall traps, and 1 branchfall
159 collection tarp, resulting in 154 soil respiration collars, 96 litterfall traps, and 48
160 branchfall collection tarps within the 1 km^2 footprint around the flux tower. We followed
161 established methods for estimating woody biomass and production (Clark et al., 2001;
162 Curtis, 2008), litterfall and branchfall (Bernier et al., 2008), and biomass of coarse woody
163 debris (Valentine et al., 2008).

164 In each of the 48 subplots within the 1 km^2 footprint of the flux tower the
165 location, diameter at breast height (dbh), and species of all trees greater than 12.7 cm
166 were recorded annually from 2004-2016. For small trees (2.54 to 12.7 cm dbh), all trees
167 were measured within a 2 m radius microplot within each subplot, with microplot center
168 4 meters (at an azimuth of 90^o) from subplot center. Dbh measurements on all trees were

made each year after leaf fall in late October/early November by the same three person team using paint markings to improve the consistency of repeat measurements.

To calculate the NPP of live woody tissues (both large and small trees), estimates of live woody biomass of the previous year were subtracted from current year estimates, while holding the dbh of any trees that died throughout the study period constant at the last live measurement as recommended in Clark et al. (2001). Above and belowground woody NPP and associated uncertainty were then calculated using a Monte Carlo simulation approach similar to that described by Yanai et al. (2010). This approach estimates the statistical distribution of the output of a calculation through multiple iterations in which the input data are chosen randomly based on their underlying distributions. Specifically for each iteration the measured diameter of each tree was allowed to vary randomly with a normal distribution using standard deviation (s.d.) of 0.1 cm. The percent carbon (%C) of woody material was varied randomly for both hardwood species (mean of 48% and s.d. of 1%) and for coniferous species (mean of 50% and s.d. of 1%). Because many allometric equations lack estimates of error, we simulated uncertainty due to allometric modeling by randomly selecting between 3 different sets of allometric models. Two local species specific allometric models (Whittaker et al., 1974; Young et al., 1980), and one set of generalized (taxonomically grouped) allometric models (Chojnacky et al., 2014) were chosen randomly for each iteration. For each iteration, %C and choice of allometric model were held constant for all years. The mean and 95% confidence interval of 1000 iterations were used to derive NPP (difference between current and previous year woody biomass), and associated uncertainty measurements for each subplot for each year. Uncertainties from the Monte

Carlo simulations were propagated with spatial (plot to plot) and temporal variability using classical error propagation techniques (see Section 2.6.).

Annual branchfall collections were used to calculate a mean estimate of the contribution of branchfall to woody carbon flux, while annual foliar and fruit/flower collections were used to calculate a mean estimate of carbon flux to foliar/fruit/flower production. Branchfall (<5 cm diameter) was collected once per year in October, using one 3.34 m^2 branchfall tarp on each subplot for a total of 48 branchfall tarps. Annual foliar and fruit/flower production were estimated by collection of aboveground litterfall using 2 litterfall traps (0.24 m^2) randomly placed in each subplot. Litter was collected 2-5 times each fall and once the following spring. To convert branchfall and litterfall into C fluxes, annual biomass collections were multiplied by the mean %C (49%). Uncertainty due to %C, spatial variability, and temporal variability were summed using standard error propagation techniques (using a 2% standard error for %C) and reported as 95% confidence intervals.

The contribution of understory production to total NPP was estimated using allometric models and annual seedling surveys on 2 meter diameter microplots in each of the 48 subplots, following methods described in (Chojnacky and Milton, 2008). Uncertainty due to spatial and temporal variation as well as uncertainties in %C were propagated using standard techniques.

2.3.2. Belowground production

Production of fine roots (<2 mm diameter) was estimated using ingrowth cores. Within the tower footprint, 90 individual year-long (late October 2013 – late October 2014) cores were installed to 30 cm depth. Total root mass per area found in the ingrowth cores was

assumed to represent annual fine root production. Estimates were not corrected for the tendency of cores to overestimate root biomass or to account for root growth below 30 cm depth. Omitting these two biases likely has a small effect on estimates of root production; Park et al. (2007) found that in stands at Bartlett Experimental Forest cores tended to overestimate by 27% (compared to soil pits) while sampling to only 30 cm led to a 28% underestimate of root biomass. Uncertainty due to spatial variation and %C (49% ± 2%), were propagated using standard error propagation techniques.

Estimates of ectomycorrhizal (ECM) fungal production were made using a stable isotope approach described in (Hobbie and Hobbie, 2008; Ouimette et al., 2013). Briefly, ECM fungi discriminate against ^{15}N during the creation of nitrogen (N) transfer compounds for plant hosts. The fraction of nitrogen transferred to ECM hosts (Tr) can be calculated (eq. 1), using the fractionation factor during mycorrhizal transfer of N (Δf), and the ^{15}N:^{14}N ratios (expressed as $\delta^{15}N$) in plant ($\delta^{15}N_{Plant}$) and soil available N ($\delta^{15}N_{Avail}$).

$$Tr = 1 + (\delta^{15}N_{Plant} - \delta^{15}N_{Avail})/\Delta f \quad (1)$$

The amount of C allocated to ECM fungal biomass can then be calculated stoichiometrically (eq. 2) using the fraction of N transferred to plant host (Tr), plant host N demand, and the C:N ratio of fungi as:

$$NPP_{fungi} = (1/Tr - 1) \times N_{demand} \times C/N_{fungi} \times f_{ECM} \quad (2)$$

where N_{demand} is annual plant N demand, C/N_{fungi} is the C/N ratio of ECM fungi, and f_{ECM} is the biomass fraction of ECM trees within the stand. Here we used the $\delta^{15}N$ of co-located (by depth) root and soil samples to calculate Tr, net annual changes in foliar, wood, and fine root N stocks to calculate plant N demand.

As an alternative approach to assess our estimates of mycorrhizal production we compared biometric estimates of NEP to estimates of NEP from eddy covariance and C inventory approaches. Specifically, production of mycorrhizal fungi was initially included as a component of NEP_B (NEP_B was calculated as total NPP minus the heterotrophic portion of ecosystem respiration – Table 1). We additionally calculated NEP_B omitting our measured mycorrhizal fungal C flux. To do this we ran Monte Carlo simulations (10,000 iterations) to calculate NEP_B, allowing estimates of each component of NPP and Rh to vary with their measured/estiamted distributions (similar to Yanai et al., 2010). Estimates of NEP_B that both included and omitted our estimate of mycorrhizal NPP were compared to NEP estimates from eddy covariance and C inventory approaches.

Additionally, we estimated total belowground carbon allocation (TBCA) using the mass balance approach described in Raich and Nadelhoffer (1989) and Davidson et al. (2002). Specifically, TBCA was estimated as the difference between total soil respiration and fine litterfall. This approach assumes that changes in the stocks of soil organic matter, roots, and litter are in near steady state or small relative to soil respiration and litterfall.

2.3.3. Soil respiration

Soil respiration was measured using infra-red gas analyzers (IRGA) in conjunction with both static chambers and autochambers. The static chambers consisted of a 10 inch PVC collar permanently inserted ~5 cm into the soil. Three collars per subplot (144 chambers across the 1 km^2 tower footprint) were measured roughly every 3 weeks during the snow-free portion of each year using a LICOR 820 CO_2 gas analyzer during 2004-2007 (>3400 measurements). Simultaneous soil moisture and temperature measurements were made at 5 cm soil depth. Chamber volumes were measured every year but were approximately 5.5 liters. After scrubbing the chamber to ~30 ppm below ambient CO_2 concentrations, concentrations were measured every 2 seconds over a 60 second period. The flux was calculated as follows: flux (umoles CO_2 m^{-2} sec^{-1}) = PV/RTA * ($dxCO_2/dt$), where P is chamber pressure in bar, V is chamber volume in m^3, T is chamber air temperature in Kelvin, A is chamber area in m^2, R is the ideal gas law constant or 0.0000834472 $m^3 \cdot bar\ K^{-1} \cdot mole^{-1}$, and ($dxCO_2/dt$) is the rate of change of the mole fraction CO_2 concentration in the chamber (umoles sec^{-1}).

During 2007-2008 five autochambers were operated on a single plot continuously during the snow-free periods of the year (>5600 measurements) following methods described in (Phillips et al., 2010).

To derive annual soil CO_2 flux estimates for both static and autochambers, measured CO_2 flux rates from the chambers were fit using a Gauss-Newton optimization method in JMP 13.0 statistical software (SAS 2016), to a suite of respiration models (Richardson et al., 2006) including Q_{10} temperature, temperature and time varying Q_{10}, soil water content modulated Q_{10}, Arrhenius, and logistic response functions. For most models, fit parameters did not vary significantly between years for either static or

283 autochambers (results not shown), thus measurements from all years were pooled to
284 derive modeled parameters for each chamber type.
285 Model best fits (using data from 2004-2008) were applied to continuous (every 30
286 min) temperature and moisture measurements made at the base of the eddy covariance
287 flux tower (5 cm depth) to estimate annual soil CO_2 flux rates for each chamber type
288 during all years (2004-2016). Lower and upper 95% confidence intervals were estimated
289 for each model and chamber type. Since annual CO_2 flux rates and model goodness of fit
290 varied minimally among model types, results from a logistic fit are reported to minimize
291 gap-filling artifacts between chamber-based soil respiration and eddy covariance tower-
292 based ecosystem respiration estimates (also modeled logistically).
293 Soil CO_2 flux during winter months was estimated using the logistic fit (above),
294 derived from measurements during the snow-free season. Because winter respiration
295 fluxes can be similar in magnitude to NEP, a more direct estimate of wintertime
296 respiration was also made during the winter of 2011-2012 using the soda lime technique
297 described in Grogan (1998) and Keith and Wong (2006). Briefly, roughly 800 g of oven-
298 dried, soda lime were left from November 17, 2011 to March 21, 2012 (125 days), in an
299 enclosed chamber (surface area = 0.06783 m^2). All post-collection soda lime weights
300 were blank-corrected using the mean of 6 field blanks prior to flux calculation. Because
301 estimates of winter respiration using the soda lime technique (data not shown) were
302 similar to those estimated using a logistic fit from chamber measurements, soil CO_2 flux
303 during winter months was estimated using the logistic temperature response model
304 described above.

To scale up to the forest stand, chamber-based soil CO_2 flux measurements were corrected for the area occupied by rocks and tree root crowns (roughly 13%) similar to Bae et al. (2015). Uncertainty was estimated by propagating uncertainty due to soil rockiness, model fit, as well as spatial and temporal variability.

2.3.4. Partitioning Rs into autotrophic and heterotrophic components

No attempt was made to directly measure the contribution of autotrophic (R_{SA}) or heterotrophic (R_{SH}) respiration to total soil respiration (R_S). Instead we used several different approaches to partition R_S. First, the Global Database of Soil Respiration Version 3 (Bond-Lamberty and Thomson, 2014) was used to derive a relationship between R_{SH} and R_S. We used data from non-experimentally manipulated, temperate, deciduous, forest ecosystems with quality check flags of Q0, Q01, Q02, and Q03 (n = 114) to derive the following relationship between annual R_{SH} and R_S: $R_{SH} = 1.925 (\pm 34.392) + R_S * 0.534 (\pm 0.045)$. This relationship was used with measured estimates of mean annual R_S to derive annual estimates of R_{SH} (and R_{SA} by difference). Monte Carlo simulations using the uncertainty in annual R_S and in the relationship between R_S and R_{SH} were used to estimate uncertainty in R_{SH} and R_A and reported as 95% confidence intervals as described above. As an additional approach to help assess the uncertainty in estimates of R_{SH}, we estimated R_{SH} independently by summing all detritus inputs (branchfall, foliar litterfall and root and mycorrhizal production) following (Bond-Lamberty et al., 2004). This independent approach was compared to estimates of R_{SH} using the portioning method described above.

2.3.5. Respiration from woody biomass

To estimate annual respiratory losses from dead woody material, estimates of dead woody C stocks were multiplied by the mean decay rate for hardwood species from Russell et al. (2014) (hardwood species comprised 97% of the standing dead woody biomass pool). Dead woody biomass was assumed to have 49% C (Thomas and Martin, 2012) with a standard error of 2%. Uncertainty due to initial estimates of dead woody biomass, %C, and decay rates from Russell et al. (2014) were propagated using standard error propagation techniques and reported as 95% confidence intervals.

No direct measurements of respiration from live woody biomass were made. Instead, we used two approaches to estimate losses of CO_2 from live woody biomass. First, to derive a "biometric" estimate that was independent of eddy covariance measurements, live woody respiration was assumed to be equal to 0.118 of biometric GPP, the median ratio of woody respiration to GPP of mature and old growth forests (> 50 years old; n = 16) reported in the database of (Litton et al., 2007). Uncertainty was reported as 0.75 of the mean annual flux.

Additionally, we derived estimates of aboveground respiration (including foliage and live and dead woody biomass) as the annual difference between eddy covariance estimates of ecosystem respiration and soil respiration from chamber measurements.

2.3.6. Foliar respiration

Dark respiration for live foliage was estimated using species-specific leaf-level measurements of dark respiration and scaled to the stand and annual scales using estimates of stand leaf area index (LAI) and a temperature sensitive Q_{10} response function. Specifically, gas exchange measurements of dark respiration were conducted

during August of 2014 and July/August of 2016 on cloud-free days between 1000 - 1500 EST using a portable gas exchange system (LICOR-6400xt, LICOR, Lincoln, NE, USA), equipped with a standard 2 × 3 cm leaf cuvette and a LICOR-6400-02B LED light source. During measurements [CO_2] was maintained at a value of 400 ppm, relative humidity at 50%, and temperature held constant at a temperature of 24.5°C (reference temperature). Species-specific estimates of foliar dark respiration (n=75 across all species) were then weighted by the fractional contribution of each species to stand LAI to derive a stand-level dark respiration rate at the reference temperature (Rd_{ref}).

A Q10 response function (eq. 3) was used to estimate dark respiration rates at temperatures other than the reference temperature using Rd_{ref} and half hourly measurements of air temperature (periods when PAR < 5 umoles m^{-2} sec^{-1}), where for eq. 3, Tair and Tref, were the measured air temperature and reference air temperature (24.5^{o}C), respectively.

$$\text{Foliar dark respiration rate} = Rd_{ref} \times Q10^{(Tair - Tref)} \quad (3)$$

Because the Q10 temperature response function of foliar dark respiration is known to vary over short timescales with changes in ambient temperature, Q10 was allowed to vary with ambient temperature following (Tjoelker et al., 2001; Q_{10} = 3.22 – 0.046 * air temperature). Annual stand-level foliar dark respiration rates were then made by multiplying temperature adjusted dark respiration rates by estimates of stand LAI summing half hourly estimates.

371 Uncertainty due to variation in leaf-level dark respiration rates, as well as
372 uncertainty in estimates LAI and the temperature response function reported in (Tjoelker
373 et al., 2001) were quantified using Monte Carlo simulations as described above where
374 estimates of each parameter were allow vary with their measured distributions.
375

376 ## 2.4. Changes in carbon stocks (ΔC)

377 To complement eddy covariance and biometric estimates of NEP, we estimated the mean
378 annual change in total ecosystem carbon stocks (ΔC) using a modified carbon inventory
379 approach. Inventory approaches rely on knowing the carbon stock of various ecosystem
380 pools at two points in time. In closed-canopy forest stands, the pools of primary
381 importance are live and dead woody biomass, as well as soil carbon. Here we focus on
382 changes in woody carbon stocks and assume that changes in soil carbon stocks were
383 minimal as was found from measurements at mature stands in nearby Hubbard Brook
384 Experimental Forest (Yanai et al., 2013). Changes in soil carbon stocks would be very
385 difficult to detect over a 13 year study period (Vadeboncoeur et al., 2012). Instead, in
386 these mature (100-125 year old) stands we assumed that there was little to no net change
387 in annual soil C stocks; however, we included an uncertainty of ± 40 g C m^{-2} yr^{-1} (Post
388 and Kwon, 2000).
389 To estimate changes in woody carbon stocks, we used a modified inventory
390 approach. First, in 2004, we made initial measurements of standing live and dead woody
391 biomass using the allometric approach described above (Section 2.3.1), except that
392 standing dead woody biomass was adjusted using species- and decay-class specific
393 density reduction factors from Harmon et al. (2011), and structural loss adjustment

394 factors from Domke et al. (2011). In 2004 we also made estimates of dead woody
395 biomass in coarse woody debris (CWD) using field surveys. For all downed woody
396 material > 7.6 cm, estimates of CWD decay class and volume were estimated using 3
397 methods: line intersect sampling (LIS), modified transect relascope sampling (MTRS),
398 and fixed plot sampling, see Pesonen et al. (2009) and Valentine et al. (2008) for details
399 of each method type. For the present study, two 100 meter transects (LIS), one 1 meter
400 transect (MTRS), or four 1 m^2 subplots per each of the 12 FIA style plots were sampled.
401 CWD volume was then multiplied by species- and decay class- specific density values
402 from Harmon et al. (2008) to estimate CWD biomass. Total dead woody biomass in
403 2004 was estimated as the sum of CWD and standing dead pools.
404 Because we had only a single measurement of standing dead biomass and CWD
405 in 2004, we estimated changes in dead woody biomass using annual inputs to the dead
406 woody pool (from known live tree death and measured branchfall), while accounting for
407 loss of carbon through decay from standing and downed dead wood using a decay rate of
408 0.0467 (the weighted average of the rates reported in Russell et al. (2014) for hardwoods
409 and conifers based on the proportion of standing dead wood in our plots). To derive the
410 mean annual change in total ecosystem carbon stocks (ΔC) we assumed the
411 predominantly angiosperm woody biomass was comprised of 49% C with a standard
412 error of 2% (Thomas and Martin, 2012). Uncertainty due to initial estimates of dead
413 woody biomass, %C, and decay rates from Russell et al. (2014), and the assumption of no
414 changes in soil C stocks were propagated using standard error propagation techniques and
415 reported as 95% confidence intervals.

2.5. Potential drivers of interannual variability

To investigate the potential drivers of interannual variation in woody NPP, NEE, GPP, and Re, we used a suite of meteorological and phenological parameters measured at the flux tower including incoming total, direct, and diffuse photosynthetically active radiation (PAR), air and soil temperature, soil thaw day, precipitation, relative humidity, vapor pressure deficit, soil moisture content, the length, start and end dates of periods of gross and net carbon uptake, as well as the length of the vernal window - defined here as the number of days between soil thaw and the onset of gross carbon uptake (where mean daily GPP_{EC} averaged over a 7 day period, exceeded 4 umoles CO_2 m^{-2} sec^{-1}). We also calculated a drought index by counting the number of growing season days where the volumetric water content (VWC) was less than 17.5%; a value that represented 50% of the growing season mean during 2004-2016. In addition to these meteorological and phenological parameters we collected data on biochemical and biological parameters including annual concentrations of foliar nitrogen (estimated following Smith et al. (2008)) and masting years from Potter et al. (2015). Annual estimates of growing season canopy level Amax and dark respiration (R_d) from the eddy flux data were estimated using a light response curve (eq. 4). For this analysis, all high-quality (ustar-filtered, non-gapfilled) measurements of half hourly NEP during June-August were used with measured PAR to estimate model parameters (e.g. Amax, Rd).

$$NEP = \frac{a * \mathrm{PAR}}{\left(\left(1-\frac{PAR}{2000}\right)+\frac{a * PAR}{Amax}\right)} - Rd \quad (4)$$

where PAR was the measured incoming photosynthetically active radiation and *a* was the quantum yield.

Both current year and 1 year lagged annual and seasonal data from these metrics were compared to measured C fluxes using stepwise linear multiple regression analysis with AIC (Akaike information criterion) to identify significant relationships.

2.6. Statistical Methods and Uncertainty Propagation

To combine estimates of uncertainty from various sources (e.g. temporal, spatial, analytical, etc.) standard uncertainty propagation techniques were used. Specifically, to add sources of uncertainty the following approach was taken:

$$SE_{(x+y)} = \sqrt{(SE_x)^2 + (SE_y)^2} \quad (5)$$

Where SE is standard error of component x, y, or (x + y). 95% confidence intervals were then estimated as 1.96 * SE.

3. Results

3.1. Estimated carbon fluxes using multiple approaches

3.1.1. Multiyear mean fluxes

Estimates and associated uncertainties of mean ecosystem C fluxes during 2004-2016 are shown in Table 1 and include components of NPP, respiratory fluxes, and estimates of NEP, GPP, and Re. Mean (2004-2016) estimates of NEP_{EC}, NEP_B, and ΔC ranged from 120-133 g C m^{-2} yr^{-1}, indicating surprising consistency in multiyear mean estimates of ecosystem net carbon flux across top-down and bottom-up approaches. All three approaches indicate that this aging 100-125 year old stand is a moderate carbon sink. Eddy covariance and biometric estimates of mean (2004-2016) GPP and Re also differed

by less than 5% and were statistically indistinguishable. Total belowground carbon allocation (calculated as soil respiration minus fine litterfall) was estimated at 656 ± 54 g C m^{-2} yr^{-1}, within the range reported for stands of similar age within BEF (620-681 g C m^{-2} yr^{-1}) (Bae et al., 2015).

The magnitude of uncertainty in NEP, GPP, and Re differed across approaches. For estimates of NEP, eddy covariance (132 ± 49 g C m^{-2} yr^{-1}) and inventory (133 ± 34 g C m^{-2} yr^{-1}) approaches had much lower uncertainty than biometric estimates of NEP (120 ± 156 g C m^{-2} yr^{-1}). Uncertainty in eddy covariance estimates originate both from the measurements themselves as well as filtering and gapfilling procedures. Estimates of the uncertainty due to potential biases in the selection of a ustar filter were not included and would increase the reported uncertainty (Figure 2). Uncertainty in biometric estimates of NEP are largely driven by uncertainties in fine root and mycorrhizal NPP as well as the heterotrophic portion of soil respiration (17%, 36%, and 42% of total error respectively).

Because estimates of the production of mycorrhizal fungi are lacking from many forest C budget efforts, we also used Monte Carlo simulations to calculate NEP_B excluding our mycorrhizal C flux estimates, using only mean fluxes and uncertainty from the other components of NEP_B. Excluding our estimates of mycorrhizal production resulted in NEP_B near zero (-3 ± 123 g C m^{-2} yr^{-1}), and an inconsistency between NEP_B and both NEP_{EC} and ΔC.

3.1.2 Components of NPP

Mean annual NPP was estimated at 615 ± 118 g C m^{-2} yr^{-1}. Growth of woody biomass including aboveground components of large and small trees, and replacement of

480 branchfall comprised approximately 33% of total NPP (238 ± 30 g C m^{-2} yr^{-1}). Annual
481 production of foliage, fruits, flowers, and seedlings was estimated at 143 ± 15 g C m^{-2} yr^{-1}
482 or 23% of total NPP. This value may be an underestimate due to removal of seeds from
483 litter baskets by small mammals. Estimates of fine root production and production of
484 mycorrhizae were 110 ± 64 and 124 ± 93 g C m^{-2} yr^{-1}, respectively, and, along with
485 coarse woody roots, resulted in a belowground production estimate that was 44% of total
486 NPP. Uncertainties in estimated belowground C fluxes to mycorrhizae are unknown, but
487 are likely to be large. If we set this value at 75% of our measured estimate, then
488 uncertainties in belowground fluxes (including fine root production) accounted for 94%
489 of the uncertainly in total NPP.

490 **3.1.3. Respiratory Fluxes**

491 Estimates of autotrophic and heterotrophic components of soil CO_2 flux, as well as
492 respiration from woody biomass and foliage are shown in Table 1. Soil respiration
493 represented the largest component of ecosystem respiration at 810 ± 48 g C m^{-2} yr^{-1}.
494 Estimates of soil respiration from manual chambers and autochambers were within 5% of
495 one another and annual estimates were relatively insensitive to the type of model used to
496 scale instantaneous measurements to annual fluxes (data not shown). Modelled winter
497 fluxes from manual and autochambers were similar to estimates over the same time
498 period using a soda lime technique (data not shown). Annual soil respiration estimates
499 are also within the range estimated at similar stands elsewhere within the Bartlett
500 Experimental Forest (790-864 g C m^{-2} yr^{-1}; Bae et al., 2015).

501 The heterotrophic portion of soil respiration (using the partitioning approach
502 described above) was estimated at 434 ± 101 g C m^{-2} yr^{-1}, and was the largest

503 heterotrophic component of ecosystem respiration. In comparison, independent estimates
504 of R_{SH} from summing inputs of detritus were 388 g C m^{-2} yr^{-1}. This value is within the
505 uncertainty but lower than our estimates of R_{SH} using the partitioning approach. In the
506 ecosystem is roughly in steady state with regards to soil inputs and outputs, then
507 estimates of R_{SH} made by summing detrital inputs are likely underestimates because they
508 exclude inputs from incorporation of CWD and root exudates. Heterotrophic respiration
509 from aboveground dead woody biomass was estimated at 61 ± 12 g C m^{-2} yr^{-1}.

510 The autotrophic portion of soil respiration was the largest component of
511 autotrophic ecosystem respiration (55%) at 376 ± 101 g C m^{-2} yr^{-1}. Autotrophic
512 respiration from foliage and live woody material together make up 45% of total
513 autotrophic respiration, estimated at 149 ± 20 and 153 ± 114 g C m^{-2} yr^{-1}, respectively.

514 Measurements of the components of ecosystem respiration include soil respiration
515 as well as aboveground foliar and woody respiration. We had measurements for total soil
516 respiration and foliar respiration but lacked direct measurements of respiration from
517 aboveground woody material. To assess the consistency of our estimates of aboveground
518 woody respiration with estimates of other measured carbon fluxes in this system, we
519 compared mean daily estimates of Re_{EC} to soil respiration (Rs), to estimate respiration
520 from aboveground components R_{abv}. The difference between mean annual Re_{EC} and Rs
521 was 343 g C m^{-2} yr^{-1}, or ~30% of Re_{EC} (Figure 3a). In comparison, the sum of our
522 estimates of aboveground live foliar and woody autotrophic, as well as dead woody
523 heterotrophic respiration from biometric estimates totaled 363 g C m^{-2} yr^{-1}, roughly 31%
524 of Re_{EC}.

3.2. Interannual variation and climate drivers

Considerable interannual variation in several meteorological and phenological variables occurred over the 13 year period (2004-2016) used to calculate mean C fluxes. For example, mean annual air temperature varied by nearly 2ºC, mean spring (Julian days 76-135) and early summer (Julian days 136-215) air temperatures by more than 3ºC, and mean winter air temperature by more than 6ºC. Variables related to the start of the growing season also differed significantly over the 13 year period with variations in soil thaw day of more than a month, the onset of gross carbon uptake by more than 2 weeks, and the length of the vernal window by more than 5 weeks. In addition, growing season precipitation ranged from 279 to 680 mm, while the number of growing season days with a mean volumetric water content (VWC) less than 17.5% ranged from 0 to 42 days per year.

Interannual variation in eddy covariance estimates of GPP, Re, and NEP during this 13-year period varied by ±9%, ±12%, and ±80% around their means, respectively. We used stepwise multiple regression and model averaging to identify the phenological and meteorological parameters that were most strongly related to interannual variation in C fluxes (e.g. Hui et al., 2003). Using simple regression approaches, a majority of the interannual variation in GPP_{EC} were captured using a two-parameter model ($r^2 = .83$ $p < 0.0001$) that included growing season soil temperature (negative correlation) and total incoming PAR during the growing season (positive correlation) - the two parameters that were used to parameterize the gap filling models employed for Re_{EC} and GPP_{EC}, respectively. Similarly, interannual variation in Re_{EC} was most strongly related to fluctuations in mean annual soil temperature (positive correlation).

548 Because of the predominance of gap-filled estimates in computing annual sums,
549 we took a second approach to assess potential controls on interannual C flux variability
550 using only high quality, half-hourly NEE data to parameterize a simple Michaelis-Menten
551 light-response model. Interannual variation in modelled parameter estimates of canopy
552 level maximum gross carbon uptake (Amax) and dark respiration (Rd) were regressed
553 against meteorological and phenological variables.
554 The strongest correlation with growing season (June-August) Amax, was the
555 length of the vernal window, defined here as the number of days between soil thaw and
556 the start of the C uptake period ($r^2 = 0.74$, $p < 0.00031$; Figure 4b). Taken separately, soil
557 thaw day was also significantly, positively correlated with Amax ($r^2 = 0.44$, $p = 0.019$;
558 Figure 4a), while the start of C uptake was not ($p = 0.12$). A longer vernal window (and
559 an earlier soil thaw day) was correlated with a lower canopy Amax. Adding additional
560 parameters did not result in an improved model and we did not detect a correlation
561 between Amax and previous year net or gross C uptake at annual or seasonal time scales.
562 Interannual variation in estimates of canopy-level dark respiration from the light-response
563 model was positively correlated to Amax ($r^2 = 0.69$, $p = 0.0009$), and, showed a similar
564 negative correlation with the length of the vernal window ($r^2 = 0.47$ $p = 0.0014$
565 Annual wood growth (Figure 5a) was compared to both current-year and previous
566 year meteorological and phenological variables as well as GPP_{EC} and NEP_{EC}, across a
567 range of time periods (seasons). No significant relationship was detected between annual
568 wood production and variations in gross or net carbon uptake from any time period
569 (current-year or lagged). Instead wood growth was best predicted with a two parameter
570 model that included early summer air temperature and the number of growing season

571 days with soil volumetric water content less than 17.5% (r^2 = 0.75, p < 0.002, RMSE =
572 16.9 g C m^{-2} yr^{-1}; Figure 5b), with higher wood growth rates occurring in warmer and
573 wetter years.

574 4. Discussion

575 4.1. Comparison of top-down and bottom-up approaches and
576 uncertainty using mean C fluxes

577 Any technique for quantifying ecosystem-scale carbon dynamics has both strengths and
578 limitations. Comparing top-down eddy covariance estimates of C exchange and bottom-
579 up biometric estimates of C fluxes can serve as a valuable cross-validation tool, and can
580 improve estimates of both an ecosystem's carbon balance as well as its components. At
581 BEF, differences in 13 year mean (2004-2016) estimates of NEP, GPP, and Re between
582 eddy covariance and biometric approaches were all within 10% of one another, indicating
583 surprising consistency between methods despite large difference in their underlying
584 sources of error. Consistency between eddy covariance and biometric approaches is
585 often seen when comparing multiyear mean estimates. For example, at a secondary
586 successional mixed northern hardwood forest in Michigan, the difference between NEP
587 from eddy covariance and biometric approaches varied by up to 148% for individual
588 years, but converged to within 1% of one another using 5 year mean estimates (Gough et
589 al., 2008).

590 The agreement in eddy covariance and biometric C flux estimates at BEF
591 provided confidence in estimates of difficult-to-measure C fluxes, and highlighted the
592 advantage of complementary methodological approaches. For example, the flux tower at

593 BEF is situated within a valley at 250 m above sea level, and on all sides the surrounding
594 land rises to >750 meters above sea level within 3 km of the flux tower (Figure 1). This
595 topographic relief increases the potential for advective transport of CO_2, which could lead
596 to underestimates of C exchange measured at the top of the eddy covariance flux tower.
597 Advective losses are a well-known challenge when using the eddy covariance technique
598 and have been dealt with in several ways; the most common being the application of a
599 ustar (friction velocity) threshold filter to exclude data when atmospheric turbulence is
600 not developed enough to minimize horizontal advective transport(Aubinet, 2008; Aubinet
601 et al., 2012). Following the ustar filter threshold selection approach of Barr et al. (2013),
602 the high ustar threshold determined at BEF (0.5 m s^{-1}), in addition to other data gaps
603 resulted in exclusion of >90% of available nighttime data (Figure 2). Despite this
604 tradeoff in data quantity, using only high quality, ustar filtered data, resulted in good
605 agreement with biometric approaches.
606 The use of biometric data to estimate NEP, GPP, and Re requires estimates of C
607 flux to several ecosystem pools that are extremely difficult to measure. At BEF
608 aboveground fluxes of net primary production are relatively well-constrained, while
609 belowground C fluxes to fine roots and especially mycorrhizal fungi have higher
610 uncertainty. However, not including estimates of these difficult-to-measure fluxes
611 resulted in an inconsistency between biometric and eddy covariance estimates of gross
612 and net C fluxes. In lieu of making individual estimates of fine root and mycorrhizal
613 production, a mass balance approach to estimate total belowground carbon allocation
614 (TBCA) described in (Davidson et al., 2002), can be used, although it does not
615 distinguish between fine root and mycorrhizal fungi production. This approach assumes

616 that soil carbon stocks are at or near steady state and requires only estimates of soil
617 respiration and aboveground fine litterfall. At BEF, TBCA was estimated at 656±54 g C
618 m^{-2} yr^{-1}, similar to estimates of the sum of coarse and fine root production, mycorrhizal
619 production, and soil autotrophic respiration, 644 g C m^{-2} yr^{-1}.
620 Estimates of aboveground foliar and woody respiration are also difficult to
621 constrain given their biological control and temporal heterogeneity. The difference
622 between estimates of ecosystem respiration and soil respiration is a mass balance
623 approach that can estimate respiration of aboveground ecosystem components (Giasson et
624 al., 2013). At BEF, this approach yielded similar results (343 g C m^{-2} yr^{-1}) to our initial
625 estimates of aboveground respiration (363 ± 117 g C m^{-2} yr^{-1}). This mass balance
626 approach also yields estimates at a fine temporal resolution and may capture important
627 phenological events (Davidson et al., 2006). At BEF estimates of R_{abv} using this mass
628 balance approach highlight the phenological influence on aboveground respiration, with
629 R_{abv} contributing a relatively large proportion of Re during spring leaf out (and the onset
630 of wood growth) and during autumn leaf senescence (Figure 3b).
631 The consistency of our initial C flux estimates with mass balance approaches that
632 used soil respiration, aboveground litterfall, and Re_{EC} to calculate TBCA and R_{abv},
633 demonstrate the benefit of including these as routine data streams at eddy covariance
634 network sites. Including soil respiration and litterfall measurements at flux sites provides
635 valuable information on both above and belowground ecosystem C fluxes allowing for
636 not only cross validation of ecosystem C fluxes but the ability to more rigorously test
637 ecosystem models (McFarlane et al., 2014; Phillips et al., 2017).

4.2. Interannual variation

4.2.1 GPP, Re, Amax

Interannual variations in GPP, Re, NEP, and parameters describing light response functions are determined by both direct and indirect drivers, and have the potential to provide insight into how ecosystems might respond under future climate. A complication in understanding the drivers of interannual C variation from eddy covariance is the abundance of gap-filled data. At BEF, on average, 90-95% of nighttime and nearly 50% of daytime fluxes during the growing season were gap-filled. It is thus not surprising that interannual variation in gap-filled GPP_{EC} and Re_{EC} were strongly related to temperature and incoming PAR, the two variables used to parameterize the gap-filling models.

Although short term (hours to days) changes in temperature and PAR are frequently correlated to short term variations in C fluxes (and hence why they are used in gap-filling models), they may not be directly related to interannual variation in C fluxes. Several studies have shown the importance of variation in the biotic response to abiotic drivers, especially for regulating interannual carbon flux variation (Richardson et al., 2007). Data from BEF support a similar conclusion. For example, using only high-quality, raw (not gap-filled) data, the strong relationship between growing season canopy Amax (and Rd) and the length of the vernal window suggests that indirect mechanisms (biotic responses) are important in regulating canopy C exchange.

Mechanisms through which the length of the vernal window can influence canopy photosynthesis are not well understood. In the northeastern US, a longer vernal window has been correlated to winters with a reduced snowpack (Contosta et al., 2016). Other studies have repeatedly linked reduced snowpack to an increase in soil freeze-thaw events

and increases in the loss of nutrients through both dissolved and gaseous pathways (Matzner and Borken, 2008; Song et al., 2017). For example, at the Hubbard Brook Experimental Forest (40 km west of BEF), both experimental (Campbell et al., 2014; Fitzhugh et al., 2001) and observational studies across a climate gradient (Durán et al., 2016) have shown increased losses of nitrogen and decreased N availability following winters with reduced snowpack. Whether decreases in soil nutrient availability prior to leaf out results in decreased foliar biomass, lower canopy nitrogen content, or reduced photosynthetic capacity is still unknown. However, leaf area index (LAI) is often limited by soil nutrients and water (Cowling and Field, 2003), and numerous studies have shown significant increases in foliar biomass and LAI following fertilization, e.g. Gower et al. (1992).

In addition to reductions in nutrient availability, earlier snowmelt has been shown to intensify forest hydrological cycles and increase springtime runoff (Creed et al., 2015). Late growing season water stress related to earlier snowmelt has also been suggested as the driver of decreases in peak growing season productivity in boreal forests (Buermann et al., 2013) and temperate forests of the western US (Hu et al., 2010). At BEF the length of the vernal window is negatively correlated to soil moisture during the month prior to leaf out ($r^2 = 0.40$, $p = 0.027$) but not to soil moisture during the late growing season ($r^2 = 0.17$, $p = 0.16$). Although mechanisms relating growing season Amax to the length of the vernal window are not fully known, data from BEF suggest that winter and spring conditions can exert a strong influence over ecosystem C dynamics during the growing season.

A few studies in temperate forests have found lagged effects on C fluxes (e.g. Howland Experimental Forest, Maine; (Richardson et al., 2013)). At BEF we did not detect a correlation between prior year meteorological conditions or C uptake, with current year C fluxes. In other work at BEF, Carbone et al., (2013) found that in stem wood of *Acer rubrum* trees, the nonstructural carbohydrate pool included both fast (younger) and slow (older) cycling subpools that could support growth and respiration of woody tissues. The lack of a correlation we see between wood growth and prior year climate and C fluxes may in part be the result of the growth habit of foliage of tree species at BEF. At BEF foliage and new shoots of the majority of the dominant species within the flux tower footprint have an indeterminate growth habit, meaning that during and after spring leaf expansion from the winter bud, the shoot apex remains active and continues to initiate additional leaves and shoot internodes if conditions are favorable. Of the dominant species only American beech and sugar maple tend to have determinate type foliar and shoot growth, where the number of leaf buds (number of leaves) is determined at the end of the preceding growing season. Many ecosystem models allocate C to foliar growth based more on a determinant type growth.

4.2.2. Wood growth

Despite the importance of wood growth for a variety of ecosystem services, we still do not fully understand the mechanisms controlling variability in wood growth and how they may respond under future climate scenarios. Evidence from broad-scale analyses suggest a tradeoff between C allocation to wood versus fine roots, reflecting a tradeoff between acquiring growth limiting nutrients and/or water and competition for space in the sunlit

canopy (Dybzinski et al., 2011; Litton et al., 2007). Whether this tradeoff at ecosystem scales occurs interannually within an ecosystem is unknown.

Alternatively, wood growth is often viewed as "source" (C supply) versus "sink" (C demand) limited (Körner, 2015). At broad spatial scales wood growth generally correlates to GPP (Litton et al., 2007). This is why wood growth in many terrestrial ecosystem models is primarily source-driven, where wood production is linked to the amount of gross photosynthesis. However, recent work has downplayed the importance of C source in controlling wood growth and has emphasized the importance of climatically sink-driven metabolic and phenological processes (Delpierre et al., 2016, 2015; Guillemot et al., 2015; Körner, 2003). These studies indicate an earlier onset of xylogenesis, faster rates of cell division, and faster rates of cell division under warmer, wetter conditions.

Our inability to detect a correlation between wood growth and either GPP or NEP at BEF suggests that interannual variations in wood growth are likely not directly "source driven." Instead, wood growth is more strongly related to early growing season air temperature and growing season soil water stress. At BEF, wood growth was higher during years with warmer air temperatures during the early growing season and in years with ample growing season soil moisture, consistent with metabolic/phenologically "sink" driven mechanisms. Further, at BEF Carbone et al. (2013) showed the importance of stored C to the growth and metabolism of woody biomass, indicating that C allocated towards wood growth relies on both recent photosynthate as well as internal reserve C pools derived from both older and recent photosynthates. At broad-scales allocation to wood growth is likely controlled by C source (GPP) as well as tradeoffs involved in

acquiring growth limiting nutrients, while metabolically driven mechanisms may be important in regulating interannual variability within a site.

5. Conclusion

Long-term datasets using multiple approaches to estimate ecosystem carbon fluxes can provide cross validation of difficult-to-measure fluxes as well as potential insight into mechanisms that may be regulating C fluxes. At BEF, top-down and bottom-up approaches to estimate gross and net C exchange agreed well at a multiyear scale and provided more confidence in several difficult-to-measure C fluxes such as aboveground components of ecosystem respiration and belowground allocation to mycorrhizal fungi. The results from BEF also suggest several potential relationships that may be important to understanding forest ecosystem C fluxes under future climate. These include potential indirect effects of winter and spring climate (vernal window) on growing season photosynthesis, as well as direct metabolic (sink-driven) mechanisms driven by growing season climate. Such mechanisms warrant future study to assess their importance and to allow for their potential inclusion in models aimed at predicting ecosystem C dynamics under future conditions.

Acknowledgements

Research at the Bartlett Experimental Forest is supported by the USDA Forest Service's Northern Research Station. We acknowledge funding support from the following grants: National Science Foundation awards #DEB-1114804, #1638688, and # 1114804; Northeastern States Research Cooperative #12DG11242307065; Hubbard Brook Long Term Ecological Research program, NSF 1114804; NH EPSCoR Program NSF Research

Infrastructure Improvement Award # EPS 1101245; NASA Carbon Cycle Science Awards #NNX08AG14G and #NNX14AJ18G; NASA Terrestrial Ecology Award #NNX11AB88G. TFK was supported by the Director, Office of Science, Office of Biological and Environmental Research of the US Department of Energy under Contract DE-AC02-05CH11231 as part of the RGCM BGC-Climate Feedbacks SFA. We also acknowledge the staff at Bartlett Experimental Forest, in particular Chris Costello, as well as the invaluable assistance of numerous students over the last 13 years.

Citations

Aubinet, M., 2008. Eddy Covariance Co2 Flux Measurements in Nocturnal Conditions: An Analysis of the Problem. Ecol. Appl. 18, 1368–1378. https://doi.org/10.1890/06-1336.1

Aubinet, M., Feigenwinter, C., Heinesch, B., Laffineur, Q., Papale, D., Reichstein, M., Rinne, J., Gorsel, E.V., 2012. Nighttime Flux Correction, in: Aubinet, M., Vesala, T., Papale, D. (Eds.), Eddy Covariance, Springer Atmospheric Sciences. Springer Netherlands, pp. 133–157. https://doi.org/10.1007/978-94-007-2351-1_5

Bae, K., Fahey, T.J., Yanai, R.D., Fisk, M., 2015. Soil Nitrogen Availability Affects Belowground Carbon Allocation and Soil Respiration in Northern Hardwood Forests of New Hampshire. Ecosystems 1–13. https://doi.org/10.1007/s10021-015-9892-7

Barr, A.G., Black, T.A., Hogg, E.H., Kljun, N., Morgenstern, K., Nesic, Z., 2004. Inter-annual variability in the leaf area index of a boreal aspen-hazelnut forest in relation to net ecosystem production. Agric. For. Meteorol. 126, 237–255. https://doi.org/10.1016/j.agrformet.2004.06.011

Barr, A.G., Richardson, A.D., Hollinger, D.Y., Papale, D., Arain, M.A., Black, T.A., Bohrer, G., Dragoni, D., Fischer, M.L., Gu, L., Law, B.E., Margolis, H.A., McCaughey, J.H., Munger, J.W., Oechel, W., Schaeffer, K., 2013. Use of change-point detection for friction–velocity threshold evaluation in eddy-covariance studies. Agric. For. Meteorol. 171–172, 31–45. https://doi.org/10.1016/j.agrformet.2012.11.023

Bernier, P., Hanson, P.J., Curtis, P.S., 2008. Measuring Litterfall and Branchfall, in: Hoover, C.M. (Ed.), Field Measurements for Forest Carbon Monitoring. Springer Netherlands, pp. 91–101. https://doi.org/10.1007/978-1-4020-8506-2_7

Bond-Lamberty, B., Thomson, A., 2014. A global database of soil respiration data, Version 3.0. Data Set Available -Line Httpdaacornlgov Oak Ridge Natl. Lab. Distrib. Act. Arch. Cent. Oak Ridge Tenn. USA Httpdxdoiorg103334ORNLDAAC1235.

Bond-Lamberty, B., Wang, C., Gower, S.T., 2004. A global relationship between the heterotrophic and autotrophic components of soil respiration? Glob. Change Biol. 10, 1756–1766. https://doi.org/10.1111/j.1365-2486.2004.00816.x

Buermann, W., Bikash, P.R., Jung, M., Burn, D.H., Reichstein, M., 2013. Earlier springs decrease peak summer productivity in North American boreal forests. Environ. Res. Lett. 8, 024027. https://doi.org/10.1088/1748-9326/8/2/024027

Campbell, J.L., Socci, A.M., Templer, P.H., 2014. Increased nitrogen leaching following soil freezing is due to decreased root uptake in a northern hardwood forest. Glob. Change Biol. 20, 2663–2673. https://doi.org/10.1111/gcb.12532

Carbone, M.S., Czimczik, C.I., Keenan, T.F., Murakami, P.F., Pederson, N., Schaberg, P.G., Xu, X., Richardson, A.D., 2013. Age, allocation and availability of nonstructural carbon in mature red maple trees. New Phytol. 200, 1145–1155. https://doi.org/10.1111/nph.12448

Caspersen, J.P., Pacala, S.W., Jenkins, J.C., Hurtt, G.C., Moorcroft, P.R., Birdsey, R.A., 2000. Contributions of Land-Use History to Carbon Accumulation in U.S. Forests. Science 290, 1148–1151. https://doi.org/10.1126/science.290.5494.1148

Chapin III, F.S., Woodwell, G.M., Randerson, J.T., Rastetter, E.B., Lovett, G.M., Baldocchi, D.D., Clark, D.A., Harmon, M.E., Schimel, D.S., Valentini, R., Wirth, C., Aber, J.D., Cole, J.J., Goulden, M.L., Harden, J.W., Heimann, M., Howarth, R.W., Matson, P.A., McGuire, A.D., Melillo, J.M., Mooney, H.A., Neff, J.C., Houghton, R.A., Pace, M.L., Ryan, M.G., Running, S.W., Sala, O.E., Schlesinger, W.H., Schulze, E.-D., 2006. Reconciling Carbon-cycle Concepts, Terminology, and Methods. Ecosystems 9, 1041–1050. https://doi.org/10.1007/s10021-005-0105-7

Chojnacky, D.C., Heath, L.S., Jenkins, J.C., 2014. Updated generalized biomass equations for North American tree species. Forestry 87, 129–151. https://doi.org/10.1093/forestry/cpt053

Chojnacky, D.C., Milton, M., 2008. Measuring Carbon in Shrubs, in: Hoover, C.M. (Ed.), Field Measurements for Forest Carbon Monitoring. Springer Netherlands, pp. 45–72. https://doi.org/10.1007/978-1-4020-8506-2_5

Clark, D.A., Brown, S., Kicklighter, D.W., Chambers, J.Q., Thomlinson, J.R., Ni, J., 2001. Measuring net primary production in forests: concepts and field methods. Ecol. Appl. 11, 356–370. https://doi.org/10.1890/1051-0761(2001)011[0356:MNPPIF]2.0.CO;2

Contosta, A.R., Adolph, A., Burchsted, D., Burakowski, E., Green, M., Guerra, D., Albert, M., Dibb, J., Martin, M., McDowell, W.H., Routhier, M., Wake, C., Whitaker, R., Wollheim, W., 2016. A longer vernal window: the role of winter coldness and snowpack in driving spring transitions and lags. Glob. Change Biol. n/a-n/a. https://doi.org/10.1111/gcb.13517

Cowling, S.A., Field, C.B., 2003. Environmental control of leaf area production: Implications for vegetation and land-surface modeling. Glob. Biogeochem. Cycles 17, 1007. https://doi.org/10.1029/2002GB001915

Creed, I.F., Hwang, T., Lutz, B., Way, D., 2015. Climate warming causes intensification of the hydrological cycle, resulting in changes to the vernal and autumnal windows in a northern temperate forest. Hydrol. Process. 29, 3519–3534. https://doi.org/10.1002/hyp.10450

Curtis, P.S., 2008. Estimating Aboveground Carbon in Live and Standing Dead Trees, in: Hoover, C.M. (Ed.), Field Measurements for Forest Carbon Monitoring. Springer Netherlands, pp. 39–44. https://doi.org/10.1007/978-1-4020-8506-2_4

Davidson, E.A., Richardson, A.D., Savage, K.E., Hollinger, D.Y., 2006. A distinct seasonal pattern of the ratio of soil respiration to total ecosystem respiration in a spruce-dominated forest. Glob. Change Biol. 12, 230–239. https://doi.org/10.1111/j.1365-2486.2005.01062.x

Davidson, E.A., Savage, K., Bolstad, P., Clark, D.A., Curtis, P.S., Ellsworth, D.S., Hanson, P.J., Law, B.E., Luo, Y., Pregitzer, K.S., Randolph, J.C., Zak, D., 2002. Belowground carbon allocation in forests estimated from litterfall and IRGA-based soil respiration measurements. Agric. For. Meteorol., FLUXNET 2000 Synthesis 113, 39–51. https://doi.org/10.1016/S0168-1923(02)00101-6

Delpierre, N., Berveiller, D., Granda, E., Dufrêne, E., 2016. Wood phenology, not carbon input, controls the interannual variability of wood growth in a temperate oak forest. New Phytol. 210, 459–470. https://doi.org/10.1111/nph.13771

847 Delpierre, N., Vitasse, Y., Chuine, I., Guillemot, J., Bazot, S., Rutishauser, T., Rathgeber,
848 C.B.K., 2015. Temperate and boreal forest tree phenology: from organ-scale
849 processes to terrestrial ecosystem models. Ann. For. Sci. 73, 5–25.
850 https://doi.org/10.1007/s13595-015-0477-6
851 Domke, G.M., Woodall, C.W., Smith, J.E., 2011. Accounting for density reduction and
852 structural loss in standing dead trees: Implications for forest biomass and carbon
853 stock estimates in the United States. Carbon Balance Manag. 6, 14.
854 https://doi.org/10.1186/1750-0680-6-14
855 Durán, J., Morse, J.L., Groffman, P.M., Campbell, J.L., Christenson, L.M., Driscoll, C.T.,
856 Fahey, T.J., Fisk, M.C., Likens, G.E., Melillo, J.M., Mitchell, M.J., Templer,
857 P.H., Vadeboncoeur, M.A., 2016. Climate change decreases nitrogen pools and
858 mineralization rates in northern hardwood forests. Ecosphere 7, n/a-n/a.
859 https://doi.org/10.1002/ecs2.1251
860 Dybzinski, R., Farrior, C., Wolf, A., Reich, P.B., Pacala, S.W., 2011. Evolutionarily
861 Stable Strategy Carbon Allocation to Foliage, Wood, and Fine Roots in Trees
862 Competing for Light and Nitrogen: An Analytically Tractable, Individual-Based
863 Model and Quantitative Comparisons to Data. Am. Nat. 177, 153–166.
864 https://doi.org/10.1086/657992
865 Fitzhugh, R.D., Driscoll, C.T., Groffman, P.M., Tierney, G.L., Fahey, T.J., Hardy, J.P.,
866 2001. Effects of soil freezing disturbance on soil solution nitrogen, phosphorus,
867 and carbon chemistry in a northern hardwood ecosystem. Biogeochemistry 56,
868 215–238. https://doi.org/10.1023/A:1013076609950
869 Giasson, M.-A., Ellison, A.M., Bowden, R.D., Crill, P.M., Davidson, E.A., Drake, J.E.,
870 Frey, S.D., Hadley, J.L., Lavine, M., Melillo, J.M., Munger, J.W., Nadelhoffer,
871 K.J., Nicoll, L., Ollinger, S.V., Savage, K.E., Steudler, P.A., Tang, J., Varner,
872 R.K., Wofsy, S.C., Foster, D.R., Finzi, A.C., 2013. Soil respiration in a
873 northeastern US temperate forest: a 22-year synthesis. Ecosphere 4, 1–28.
874 https://doi.org/10.1890/ES13.00183.1
875 Goodale, C.L., Apps, M.J., Birdsey, R.A., Field, C.B., Heath, L.S., Houghton, R.A.,
876 Jenkins, J.C., Kohlmaier, G.H., Kurz, W., Liu, S., Nabuurs, G.-J., Nilsson, S.,
877 Shvidenko, A.Z., 2002. Forest carbon sinks in the northern hemisphere. Ecol.
878 Appl. 12, 891–899. https://doi.org/10.1890/1051-
879 0761(2002)012[0891:FCSITN]2.0.CO;2
880 Gough, C.M., Vogel, C.S., Schmid, H.P., Su, H.-B., Curtis, P.S., 2008. Multi-year
881 convergence of biometric and meteorological estimates of forest carbon storage.
882 Agric. For. Meteorol., Chequamegon Ecosystem-Atmosphere Study Special
883 Issue: Ecosystem-Atmosphere Carbon and Water Cycling in the Temperate
884 Northern Forests of the Great Lakes RegionGreat Lakes Region Special Issue
885 148, 158–170. https://doi.org/10.1016/j.agrformet.2007.08.004
886 Gower, S.T., Vogt, K.A., Grier, C.C., 1992. Carbon Dynamics of Rocky Mountain
887 Douglas-Fir: Influence of Water and Nutrient Availability. Ecol. Monogr. 62, 43–
888 65. https://doi.org/10.2307/2937170
889 Grogan, P., 1998. Co2 flux measurement using soda lime: correction for water formed
890 during co2 adsorption. Ecology 79, 1467–1468. https://doi.org/10.1890/0012-
891 9658(1998)079[1467:CFMUSL]2.0.CO;2

892 Guillemot, J., Martin-StPaul, N.K., Dufrêne, E., François, C., Soudani, K., Ourcival,
893 J.M., Delpierre, N., 2015. The dynamic of the annual carbon allocation to wood in
894 European tree species is consistent with a combined source–sink limitation of
895 growth: implications for modelling. Biogeosciences 12, 2773–2790.
896 Harmon, M.E., Woodall, C.W., Fasth, B., Sexton, J., 2008. Woody detritus density and
897 density reduction factors for tree species in the United States: a synthesis.
898 Harmon, M.E., Woodall, C.W., Fasth, B., Sexton, J., Yatkov, M., 2011. Differences
899 between standing and downed dead tree wood density reduction factors: A
900 comparison across decay classes and tree species.
901 Hobbie, E.A., Hobbie, J.E., 2008. Natural Abundance of 15N in Nitrogen-Limited
902 Forests and Tundra Can Estimate Nitrogen Cycling Through Mycorrhizal Fungi:
903 A Review. Ecosystems 11, 815. https://doi.org/10.1007/s10021-008-9159-7
904 Hollinger, D.Y., 2008. Defining a Landscape-Scale Monitoring Tier for the North
905 American Carbon Program, in: Hoover, C.M. (Ed.), Field Measurements for
906 Forest Carbon Monitoring. Springer Netherlands, pp. 3–16.
907 https://doi.org/10.1007/978-1-4020-8506-2_1
908 Hollinger, D.Y., Aber, J., Dail, B., Davidson, E.A., Goltz, S.M., Hughes, H., Leclerc,
909 M.Y., Lee, J.T., Richardson, A.D., Rodrigues, C., Scott, N. a., Achuatavarier, D.,
910 Walsh, J., 2004. Spatial and temporal variability in forest–atmosphere CO2
911 exchange. Glob. Change Biol. 10, 1689–1706. https://doi.org/10.1111/j.1365-
912 2486.2004.00847.x
913 Hu, J., Moore, D.J.P., Burns, S.P., Monson, R.K., 2010. Longer growing seasons lead to
914 less carbon sequestration by a subalpine forest. Glob. Change Biol. 16, 771–783.
915 https://doi.org/10.1111/j.1365-2486.2009.01967.x
916 Hui, D., Luo, Y., Katul, G., 2003. Partitioning inter annual variability in net ecosystem
917 exchange between climatic variability and functional change. Tree Physiol. 23,
918 433–442.
919 Keith, H., Wong, S.C., 2006. Measurement of soil CO2 efflux using soda lime
920 absorption: both quantitative and reliable. Soil Biol. Biochem. 38, 1121–1131.
921 https://doi.org/10.1016/j.soilbio.2005.09.012
922 Körner, C., 2015. Paradigm shift in plant growth control. Curr. Opin. Plant Biol. 25, 107–
923 114. https://doi.org/10.1016/j.pbi.2015.05.003
924 Körner, C., 2003. Carbon limitation in trees. J. Ecol. 91, 4–17.
925 https://doi.org/10.1046/j.1365-2745.2003.00742.x
926 Litton, C.M., Raich, J.W., Ryan, M.G., 2007. Carbon allocation in forest ecosystems.
927 Glob. Change Biol. 13, 2089–2109. https://doi.org/10.1111/j.1365-
928 2486.2007.01420.x
929 Luyssaert, S., Schulze, E.-D., Börner, A., Knohl, A., Hessenmöller, D., Law, B.E., Ciais,
930 P., Grace, J., 2008. Old-growth forests as global carbon sinks. Nature 455, 213–
931 215. https://doi.org/10.1038/nature07276
932 Matzner, E., Borken, W., 2008. Do freeze-thaw events enhance C and N losses from soils
933 of different ecosystems? A review. Eur. J. Soil Sci. 59, 274–284.
934 https://doi.org/10.1111/j.1365-2389.2007.00992.x
935 McFarlane, K., Finzi, A., Nave, L., Tang, J., 2014. Recommendations for belowground
936 carbon data and measurements for the AmeriFlux Network [WWW Document].
937 ISCN. URL http://iscn.fluxdata.org/community/publication/recommendations-for-

938 belowground-carbon-data-and-measurements-for-the-ameriflux-network/
939 (accessed 4.18.17).
940 Novick, K., Brantley, S., Miniat, C.F., Walker, J., Vose, J.M., 2014. Inferring the
941 contribution of advection to total ecosystem scalar fluxes over a tall forest in
942 complex terrain. Agric. For. Meteorol. 185, 1–13.
943 https://doi.org/10.1016/j.agrformet.2013.10.010
944 Odum, E.P., 1969. The Strategy of Ecosystem Development. Science 164, 262–270.
945 https://doi.org/10.1126/science.164.3877.262
946 Ollinger, S.V., Smith, M.L., Martin, M.E., Hallett, R.A., Goodale, C.L., Aber, J.D., 2002.
947 Regional Variation in Foliar Chemistry and N Cycling among Forests of Diverse
948 History and Composition. Ecology 83, 339–355. https://doi.org/10.2307/2680018
949 Ouimette, A., Guo, D., Hobbie, E., Gu, J., 2013. Insights into root growth, function, and
950 mycorrhizal abundance from chemical and isotopic data across root orders. Plant
951 Soil 367, 313–326. https://doi.org/10.1007/s11104-012-1464-4
952 Park, B.B., Yanai, R.D., Vadeboncoeur, M.A., Hamburg, S.P., 2007. Estimating Root
953 Biomass in Rocky Soils using Pits, Cores, and Allometric Equations. Soil Sci.
954 Soc. Am. J. 71, 206–213. https://doi.org/10.2136/sssaj2005.0329
955 Pesonen, A., Leino, O., Maltamo, M., Kangas, A., 2009. Comparison of field sampling
956 methods for assessing coarse woody debris and use of airborne laser scanning as
957 auxiliary information. For. Ecol. Manag. 257, 1532–1541.
958 https://doi.org/10.1016/j.foreco.2009.01.009
959 Phillips, C.L., Bond-Lamberty, B., Desai, A.R., Lavoie, M., Risk, D., Tang, J., Todd-
960 Brown, K., Vargas, R., 2017. The value of soil respiration measurements for
961 interpreting and modeling terrestrial carbon cycling. Plant Soil 413, 1–25.
962 https://doi.org/10.1007/s11104-016-3084-x
963 Phillips, S.C., Varner, R.K., Frolking, S., Munger, J.W., Bubier, J.L., Wofsy, S.C., Crill,
964 P.M., 2010. Interannual, seasonal, and diel variation in soil respiration relative to
965 ecosystem respiration at a wetland to upland slope at Harvard Forest. J. Geophys.
966 Res. Biogeosciences 115, G02019. https://doi.org/10.1029/2008JG000858
967 Post, W.M., Kwon, K.C., 2000. Soil carbon sequestration and land-use change: processes
968 and potential. Glob. Change Biol. 6, 317–327. https://doi.org/10.1046/j.1365-
969 2486.2000.00308.x
970 Potter, D., Obbard, M., Howe, E., 2015. Ontario wildlife food survey, 2014. Ont. Minist.
971 Nat. Resour. For. Sci. Res. Branch Peterb. Ont. Sci. Res. Tech. Rep. TR-01.
972 Raich, J.W., Nadelhoffer, K.J., 1989. Belowground Carbon Allocation in Forest
973 Ecosystems: Global Trends. Ecology 70, 1346–1354.
974 https://doi.org/10.2307/1938194
975 Richardson, A.D., Braswell, B.H., Hollinger, D.Y., Burman, P., Davidson, E.A., Evans,
976 R.S., Flanagan, L.B., Munger, J.W., Savage, K., Urbanski, S.P., Wofsy, S.C.,
977 2006. Comparing simple respiration models for eddy flux and dynamic chamber
978 data. Agric. For. Meteorol. 141, 219–234.
979 https://doi.org/10.1016/j.agrformet.2006.10.010
980 Richardson, A.D., Carbone, M.S., Keenan, T.F., Czimczik, C.I., Hollinger, D.Y.,
981 Murakami, P., Schaberg, P.G., Xu, X., 2013. Seasonal dynamics and age of
982 stemwood nonstructural carbohydrates in temperate forest trees. New Phytol. 197,
983 850–861. https://doi.org/10.1111/nph.12042

Richardson, A.D., Hollinger, D.Y., 2007. A method to estimate the additional uncertainty in gap-filled NEE resulting from long gaps in the CO2 flux record. Agric. For. Meteorol. 147, 199–208. https://doi.org/10.1016/j.agrformet.2007.06.004

Richardson, A.D., Hollinger, D.Y., Aber, J.D., Ollinger, S.V., Braswell, B.H., 2007. Environmental variation is directly responsible for short- but not long-term variation in forest-atmosphere carbon exchange. Glob. Change Biol. 13, 788–803. https://doi.org/10.1111/j.1365-2486.2007.01330.x

Russell, M.B., Woodall, C.W., Fraver, S., D'Amato, A.W., Domke, G.M., Skog, K.E., 2014. Residence Times and Decay Rates of Downed Woody Debris Biomass/Carbon in Eastern US Forests. Ecosystems 17, 765–777. https://doi.org/10.1007/s10021-014-9757-5

Smith, M.-L., Hollinger, D.Y., Ollinger, S., 2008. Estimation of Forest Canopy Nitrogen Concentration, in: Hoover, C.M. (Ed.), Field Measurements for Forest Carbon Monitoring. Springer Netherlands, pp. 197–203. https://doi.org/10.1007/978-1-4020-8506-2_15

Song, Y., Zou, Y., Wang, G., Yu, X., 2017. Altered soil carbon and nitrogen cycles due to the freeze-thaw effect: A meta-analysis. Soil Biol. Biochem. 109, 35–49. https://doi.org/10.1016/j.soilbio.2017.01.020

Thomas, S.C., Martin, A.R., 2012. Carbon Content of Tree Tissues: A Synthesis. Forests 3, 332–352. https://doi.org/10.3390/f3020332

Tjoelker, M.G., Oleksyn, J., Reich, P.B., 2001. Modelling respiration of vegetation: evidence for a general temperature-dependent Q10. Glob. Change Biol. 7, 223–230. https://doi.org/10.1046/j.1365-2486.2001.00397.x

Vadeboncoeur, M.A., Hamburg, S.P., Blum, J.D., Pennino, M.J., Yanai, R.D., Johnson, C.E., 2012. The Quantitative Soil Pit Method for Measuring Belowground Carbon and Nitrogen Stocks. Soil Sci. Soc. Am. J. 76, 2241–2255. https://doi.org/10.2136/sssaj2012.0111

Vadeboncoeur, M.A., Hamburg, S.P., Yanai, R.D., Blum, J.D., 2014. Rates of sustainable forest harvest depend on rotation length and weathering of soil minerals. For. Ecol. Manag. Complete, 194–205. https://doi.org/10.1016/j.foreco.2014.01.012

Valentine, H.T., Gove, J.H., Ducey, M.J., Gregoire, T.G., Williams, M.S., 2008. Estimating the Carbon in Coarse Woody Debris with Perpendicular Distance Sampling, in: Hoover, C.M. (Ed.), Field Measurements for Forest Carbon Monitoring. Springer Netherlands, pp. 73–87. https://doi.org/10.1007/978-1-4020-8506-2_6

van Gorsel, E., Delpierre, N., Leuning, R., Black, A., Munger, J.W., Wofsy, S., Aubinet, M., Feigenwinter, C., Beringer, J., Bonal, D., Chen, B., Chen, J., Clement, R., Davis, K.J., Desai, A.R., Dragoni, D., Etzold, S., Grünwald, T., Gu, L., Heinesch, B., Hutyra, L.R., Jans, W.W.P., Kutsch, W., Law, B.E., Leclerc, M.Y., Mammarella, I., Montagnani, L., Noormets, A., Rebmann, C., Wharton, S., 2009. Estimating nocturnal ecosystem respiration from the vertical turbulent flux and change in storage of CO2. Agric. For. Meteorol., Special Section on Water and Carbon Dynamics in Selected Ecosystems in China 149, 1919–1930. https://doi.org/10.1016/j.agrformet.2009.06.020

Vickers, D., Irvine, J., Martin, J.G., Law, B.E., 2012. Nocturnal subcanopy flow regimes and missing carbon dioxide. Agric. For. Meteorol. 152, 101–108. https://doi.org/10.1016/j.agrformet.2011.09.004

Whittaker, R.H., Bormann, F.H., Likens, G.E., Siccama, T.G., 1974. The Hubbard Brook Ecosystem Study: Forest Biomass and Production. Ecol. Monogr. 44, 233–254. https://doi.org/10.2307/1942313

Yanai, R.D., Battles, J.J., Richardson, A.D., Blodgett, C.A., Wood, D.M., Rastetter, E.B., 2010. Estimating Uncertainty in Ecosystem Budget Calculations. Ecosystems 13, 239–248. https://doi.org/10.1007/s10021-010-9315-8

Yanai, R.D., Vadeboncoeur, M.A., Hamburg, S.P., Arthur, M.A., Fuss, C.B., Groffman, P.M., Siccama, T.G., Driscoll, C.T., 2013. From Missing Source to Missing Sink: Long-Term Changes in the Nitrogen Budget of a Northern Hardwood Forest. Environ. Sci. Technol. 47, 11440–11448. https://doi.org/10.1021/es4025723

Young, H.E., Ribe, J.H., Wainwright, K., 1980. Weight tables for tree and shrub species in Maine. Maine Life Sci. Agric. Exp. Stn. Misc. Rep. USA.

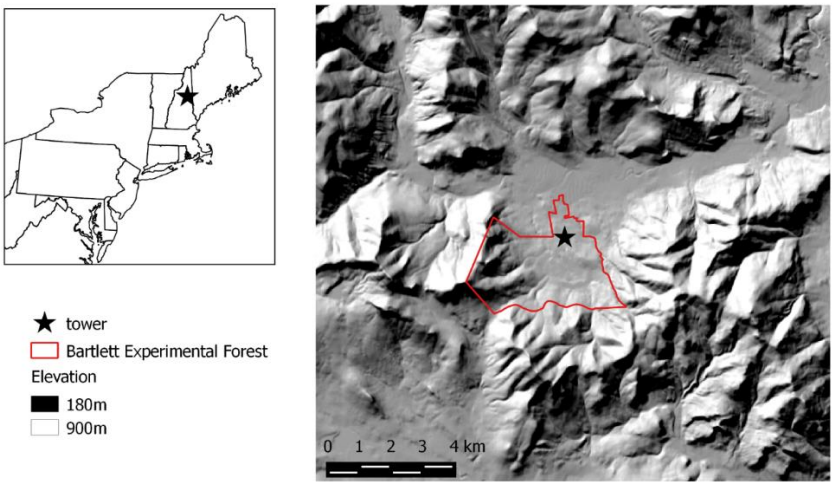

1045

1046 **Figure 1: A) Location of Bartlett Experimental Forest (BEF); B) Representation of topography**

1047 **surrounding BEF.**

1048
1049
1050

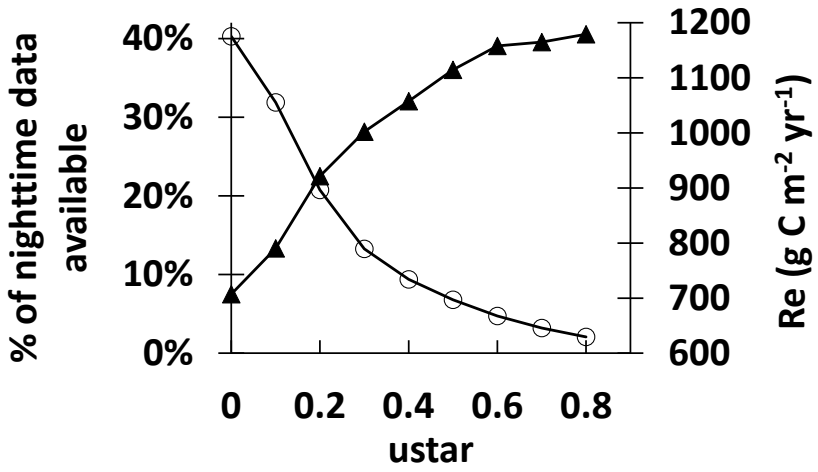

1051

1052 **Figure 2: Plot of the percent of available nighttime data during the growing season (circles) and**

1053 **mean annual ecosystem respiration (triangles) with changes in ustar, highlighting the tradeoff**

1054 **between data quantity and data quality at BEF.**

1055
1056

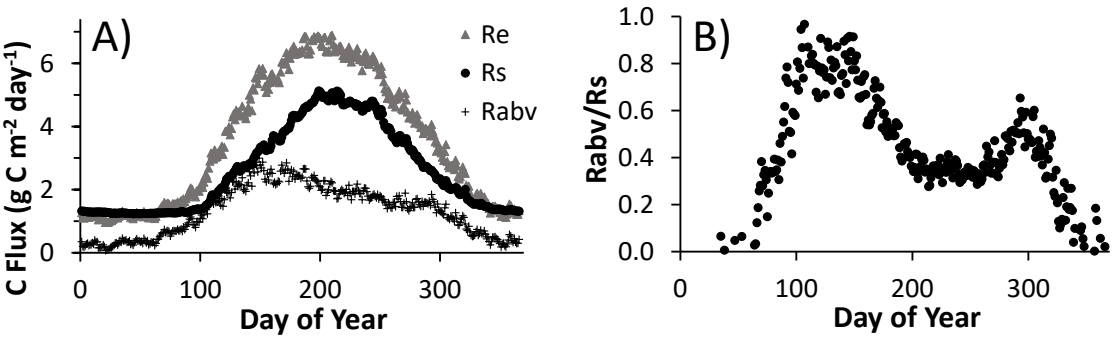

1057

1058 **Figure 3**: **A) Mean daily CO_2 flux by day of year for ecosystem respiration (Re_{EC}), soil respiration**

1059 **(Rs), and respiration from aboveground components of the ecosystem (R_{abv}); B) Ratio of R_{abv} to Rs**

1060 **by day of year.**

1061
1062
1063

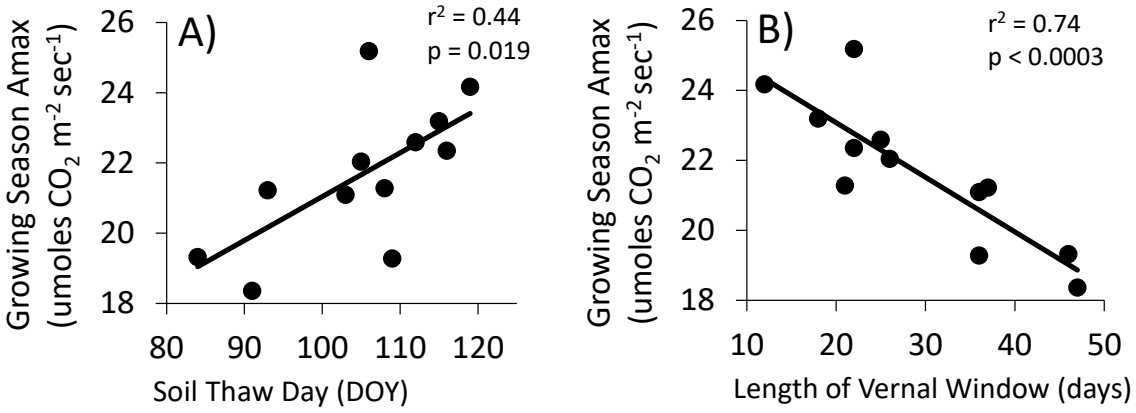

1064

1065 **Figure 4: Relationship between growing season canopy level Amax and (A) soil thaw day, and (B) the**

1066 **length of the vernal window during 2004-2016. The vernal window is defined as the number of days**

1067 **between soil thaw and the start of canopy gross carbon uptake.**

1068

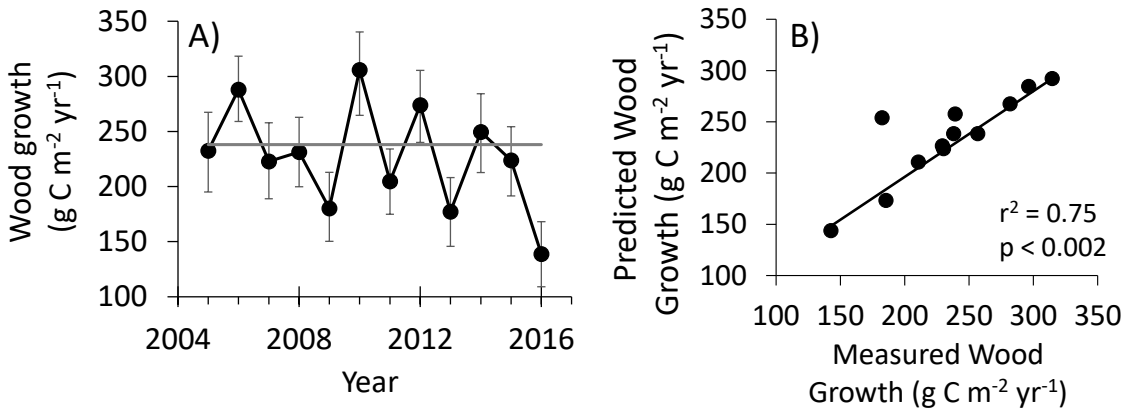

Figure 5: **A) Annual wood growth during 2004-2016 including both aboveground biomass and coarse roots. B) Predicted vs. measured wood growth. Predicted wood growth was estimated from a 2 parameter linear regression model using early summer air temperature (Julian days 136-215) and a drought index (the number of growing season days with VWC < 17.5%; 50% of the growing season mean VWC). The outlier in B) is 2013 where measured wood growth was much lower than predicted.**

1077 **Table 1: Mean carbon fluxes and uncertainty at Bartlett Experimental Forest, NH (2004-2016)**

	Components of Net Primary Production	Flux (g C m^{-2} yr^{-1})	Method
(a)	Aboveground Wood	204 ± 29	(1 + 2 + 3)
	1) Large trees (>12.7 cm dbh)	143 ± 20	Allometry; annual DBH
	2) Small trees (<12.7 cm dbh)	30 ± 5	Allometry; annual DBH
	3) branchfall	31 ± 21	Annual branchfall tarps
(b)	Foliage, fruit, flower	123 ± 11	Annual litterfall collection
(c)	Understory/herbivory	20 ± 10	Allometery on microplots
(d)	Woody roots	34 ± 7	Allometry; annual DBH
(e)	Fine roots	110 ± 64	Root ingrowth cores
(f)	Mycorrhizae	124 ± 93	Stable isotope approach
(h)	Total NPP	615 ± 118	(a + b + c + d + e + f)
	Respiratory Fluxes		
(i)	Total Soil Respiration (R_S)	810 ± 48	Manual and auto-chambers
(j)	CWD respiration	5 ± 5	CWD mass; mass loss rates
(k)	Standing dead respiration	56 ± 15	Allometry; mass loss rates
(l)	Woody autotrophic respiration	153 ± 114	0.118* GPP_B; see methods
(m)	Foliar respiration	149 ± 20	leaf level measurements
(n)	Heterotrophic Soil Respiration (R_{SH})	434 ± 101	1.92 + 0.534 * (i); see methods
(o)	Autotrophic Soil respiration (R_{SA})	376 ± 101	1 - (n)
	Ecosystem Fluxes		
	NEP_{EC}	132 ± 49	eddy covariance flux tower (-NEE)
	NEP_B	120 ± 156	NPP - $R_{h;}$ (h - j - k - n)
	ΔC	133 ± 34	modified inventory approach
	Re_{EC}	1153 ± 69	eddy covariance flux tower
	Re_B	1172 ± 127	(i + j + k + l + m)
	GPP_{EC}	1285 ± 62	eddy covariance flux tower
	GPP_B	1292 ± 194	(h + l + m + o)
	TBCA	656 ± 54	(i - b - 3)

1078

1079